International Journal of Fracture **51:** 31–42, 1991.
Z.P. Bažant (ed.), Current Trends in Concrete Fracture Research.

Tensile fracture of concrete at high loading rates taking account of inertia and crack velocity effects

H.W. REINHARDT[1] and J. WEERHEIJM[2]
[1]*Stuttgart University, Pfaffenwaldring 4, D-7000 Stuttgart 80, Germany;*
[2]*TNO Prins Maurits Laboratory, P.O. Box 45, NL-2280 AA Rijswijk, Netherlands*

Received 1 June 1990; accepted 15 November 1990

Abstract. Experiments on concrete have shown a considerable increase of apparent tensile strength with increasing loading rate. This phenomenon can be attributed to various mechanisms such as kinetics of energy barriers and inertia effects in the vicinity of a running crack. After a general introduction into the behaviour of concrete under a uniaxial tensile stress, a model is presented which accounts for flaws in concrete and the inertia effects around a crack at high loading rates. It turns out that the quite crude model predicts rather accurately the relation between apparent strength and loading rate, the influence of concrete quality on this relation, and the relation between crack propagation velocity and loading rate.

1. Introduction

Civil engineering structures are usually exposed to static loading or slowly varying loading. However, there are loading cases with high rates of loading such as impact of vehicles or planes on structures, earthquake loading, explosions and hazards. Although these are the exceptional loading cases, rather than the rule, they may be vital for the structure and for the inhabitants or users. Therefore, strength and fracture energy at high loading rate are important parameters in assessing the safety of structures.

Tensile behaviour of concrete controls cracking, minimum reinforcement ratio, shear failure of beams and slabs, bond deterioration and bond slip of steel bars in concrete, and local splitting failure. As has been shown by John and Shah [1], loading rate may be responsible for the transition of ductile bending type failure to brittle shear type failure of beams.

Although tensile strength is only one parameter which governs failure of concrete, it is a dominant one. It controls the onset of a fictitious crack according to Hillerborg [2]. According to this model, a tensile member is stressed up to the maximum stress, then deformation continues while the stress decreases. The softening causes elastic stress release of the uncracked part of the tensile member and irreversible deformation of a crack process zone. At complete stress decay, the crack borders are separated and a discrete crack has formed.

The area under the complete stress-displacement curve represents the fracture energy G_F. The ascending part of the stress-deformation line is linear to about 0.6 times the tensile strength whereafter an overproportional increase of deformation appears. The descending part is nonlinear. The shape of the line depends on the type of material and on the loading conditions [3]. G_F can be described by a function of crack opening w with the scale factor f_t which is the tensile strength

$$G_F = f_t g(w), \tag{1}$$

where g may be a bilinear or multilinear, or a continuous function of crack opening w.

In experiments on plain concrete and on steel fibre reinforced concrete, it has been shown that $g(w)$ is little affected by loading rate [4]. If $g(w)$ is taken as approximately the same for all loading rates, the rate dependence of G_F is the same as for the tensile strength. It is then sufficient to determine the tensile strength of concrete at various loading rates and to measure the complete stress-deformation curve at static loading.

2. Some aspects of fracture at high loading rates

The aforementioned relation between G_F and f_t is true for one single crack. This implies that, at high loading rates, also a single crack may occur. If multiple cracks form in the measuring length, the energy must be larger than in the case of a single crack.

There are at least three aspects which require attention: first, the bond breaking process, second, the inertia effect of the material adjacent to the crack, and third, the crack propagation velocity.

The breaking of bonds has been described by the kinetics of energy barriers (see for instance [5]). It is assumed that there is a bond breaking rate and a bond healing rate. If there is a mechanical stress applied, the breaking rate exceeds the healing rate. This causes time dependent deformation and/or cracking. Mihashi and Wittmann [6] have applied this model to concrete and found good correlation between model predictions and experiments. The rate dependence is expressed there by a power function

$$f_t/f_{t,0} = (\dot{\sigma}/\dot{\sigma}_0)^n, \tag{2}$$

with f_t and $f_{t,0}$ tensile strength at high loading rates and static loading, respectively, and $\dot{\sigma}$ the appropriate stress rates. n is a material constant with values between 0.03 and 0.06. According to this theory, the mechanism which leads to fracture is the same for all loading rates. Rigorous studies have shown that the power function expression is only valid for a moderate crack velocity [5], while higher velocities should be described by a more rigorous application of kinetics theory.

If two pieces of material are separated by a crack, they move away from each other with a certain velocity. The velocity depends on the crack propagation velocity, the compliance and mass density of the material, on the stress and, at varying stresses, on the loading rate. Kipp et al. [7] have shown that a rate dependence of tensile strength exists like

$$f_t = \beta \dot{\varepsilon}^{1/3}, \tag{3}$$

with β a material constant which depends on Young's modulus, critical stress intensity factor, and shear wave velocity. In fact, (3) is based on the effect of inertia of a single flaw under high strain rates. The applicability of the formula is confined to strain rates greater than $10^2\ s^{-1}$ for concrete assuming a flaw size of 5 mm.

Crack propagation velocity is theoretically limited to about the Rayleigh wave velocity since this is the velocity of a wave which transports energy along a surface, for instance a crack surface. However, even under high strain rates, there have been no values measured which reach this terminal velocity ([8] and [9]). While [8] reports values of about 200 m/s, [9] reports velocities of about 1000 m/s. It should be noted, however, that the value mentioned last is

determined in compressive loading tests with a less sensitive method than has been used in [8]. It seems at the moment that the crack propagation velocity of concrete is considerably lower than the Rayleigh wave speed.

If this is true, there should be an influence on the tensile strength at very high loading rates when the loading increases continuously but the crack cannot propagate fast enough. Theoretically, the apparent strength could rise without limit. Curbach [10] performed tests and carried out finite element analyses assuming a crack propagation velocity of 500 m/s. He found a steep increase of tensile strength at strain rates greater than $1\ s^{-1}$. At $\dot{\varepsilon} = 50\ s^{-1}$ the theoretical ratio between tensile strength and static tensile strength amounted to 5.

In the following section, an attempt will be made to close the gap between the three aspects which seem to be independent from each other. This model will incorporate kinetic theory and inertia effects and will predict tensile strength as a function of loading rate, and crack velocity as a function of loading time and loading rate.

3. Concrete model

Failure of concrete is determined by the fracture process. In the model the fracture process, which occurs at micro level, is characterized by the extension of schematic cracks in a fictitious fracture plane. The influence of the loading rate on the material response and the ultimate stress is reflected in crack extension and energy absorption during the pre-peak fracture process.

3.1. Schematization

The real fracture plane is represented as a plane containing uniformly distributed penny-shaped cracks. These cracks represent the damage before loading. The ratio of the initial crack diameter and the intermediate distance (a_0/b) characterizes the ratio of damaged and undamaged material (for detailed description see [11]). Figure 1 shows the planes of failure in concrete and in the corresponding model.

The geometry of the fictitious failure plane is derived from the static material properties, water cement ratio, the aggregate content along with the general feature that bond cracking starts at about 60 percent of the strength and matrix cracking at about 75 percent. During the load increase the cracks grow and dissipate the fracture energies of bond, matrix and aggregate. When the crack size equals the intermediate distance b, the strength is assumed to be reached.

The only two parameters that cannot be derived from (static) material properties and therefore must be estimated are the specific surface energies for bond and aggregates.

In the fictitious failure plane, the material between the flaws is assumed to be linear elastic. Consequently, crack extension in this plane does not describe the processes of crack arrest, crack branching or bridging of cracks. But it can reflect the influence of loading rate and geometry on average crack growth, energy absorption and thus the influence on strength.

3.2. Crack extension

During crack extension, an exchange of energy occurs between deformation energy, external work, dissipated fracture energy and kinetic energy in the material around the crack tip. The

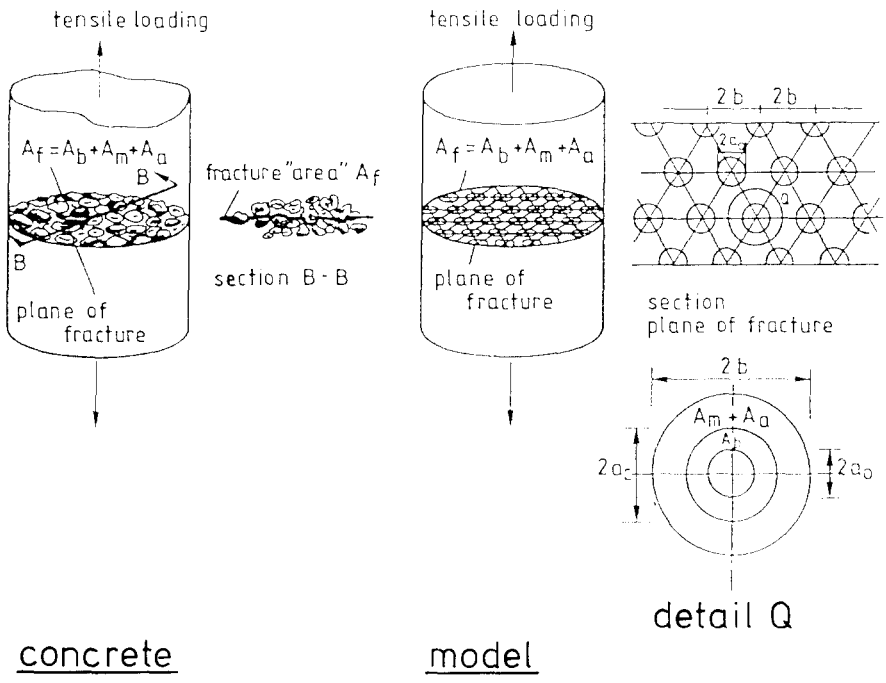

Fig. 1. Planes of fracture in concrete and model. A_b = bond area, A_m = matrix area, A_s = aggregate area, A_f = fracture area.

various energy terms can be determined if the stress, displacement and velocity fields are known. To determine these fields for dynamic loading conditions or at crack propagation, the equations of motion should be applied.

The effect of the inertia terms on the stress distribution is amongst others studied by Freund [12] and Broberg [13]. For a semi-infinite crack loaded by a longitudinal tension wave, Freund derived an expression for the dynamic stress intensity factor. The static factor should be multiplied by a function $k(\dot{a})$, which depends only on the crack velocity. It equals unity for $\dot{a} = 0$, and is reduced to zero at the limiting (Rayleigh) wave velocity (C_r).

For the geometry in the fictitious plane no analytical solution is available, but [14] and [15] showed that also for other crack geometries the velocity of crack extension is limited by the Rayleigh or shear wave velocity. Considering the force equilibrium around a crack tip this result can be argued. The reasoning is as follows. For any crack geometry the stress intensity factor will decrease when the crack tip velocity increases because the inertia components in the equilibrium become more important. A lower stress intensity means a lower energy flux into the fracture zone which causes a decrease of crack extension velocity. For any crack geometry, there must be a terminal velocity of crack extension with an equilibrium between the energy flux into the fracture zone and the energy release rate. When the terminal velocity equals C_r, the stress intensity factor must be zero because at this velocity the material around the newly formed crack surfaces cannot respond to the actual crack size and the equilibrium is realized by inertia forces. Based on these results, it can be assumed that also for the penny-shaped cracks a terminal velocity exists and that the stress intensity factor will decrease with increasing crack tip velocity.

Another aspect is that for the fictitious fracture plane the influence of the bounded geometry on the stress fields under dynamic loading is not as yet known. However a few comments are in order. First of all it must be true that also for a bounded geometry the crack tip velocity will never exceed C_r, and the dynamic stress intensity factor K_{ID} will be zero at this velocity because of the inertia effects. Second, from analytical solutions for step loadings on stable cracks, it follows that, after a certain time, the stress distribution can be described by the corresponding static stress field. The magnitude of this delay time depends on the crack size, the intermediate crack distance and the wave velocity C_r. For linear increasing loads, this result leads to a delay time in the response to the actual load level. When the time delay is supposed to be zero, the error introduced will decrease with decreasing intermediate distance and increasing fracture time, e.g. Nozaki et al. [16].

The aim of the model is not to give an exact description of the prepeak fracture process, but to characterize as simply as possible the crack extension and energy dissipation before the ultimate strength is reached. Based on this goal and the aforementioned features of crack extension, it was decided to neglect, at first, the time delay and to use the solutions from LEFM for the stress and displacement fields under static loading which are adjusted by a function $k(\dot{a})$, like Freund and Broberg [12, 13] derived, to account for inertia.

In this way, relatively simple expressions for the various energy terms are obtained and the dependency of the rate sensitivity on the various parameters can be examined. Using these adjusted solutions, the distribution of the available energy during the fracture process can be determined.

Corresponding to the approach of Mott [17] and Berry [18] and others, one considers the material around the crack tip in which the energy exchange occurs. For the penny-shaped cracks the material is bounded by the surface of a torus with radius R. The value of R is not known but should be proportional to a characteristic length parameter (see Fig. 2).

Following the approach of Mott and Berry, the integrated form of the energy balance is used:

$$-W + V + T + D = E_0, \tag{4}$$

in which E_0 equals the amount of energy inside the surface at the considered initial time t_0. W = external work, V = deformation energy, T = kinetic energy, and D = fracture energy.

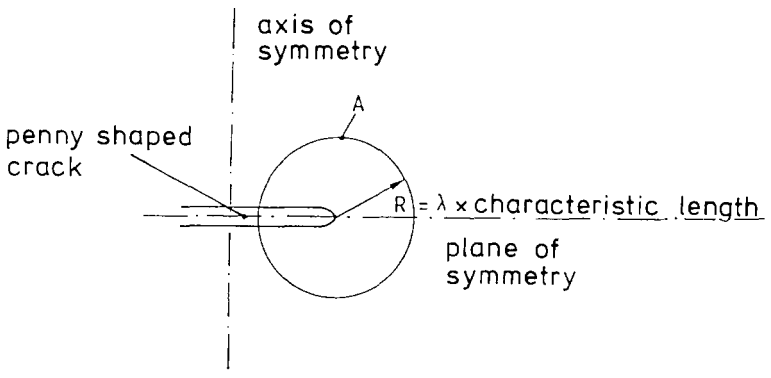

Fig. 2. The area around the crack tip. A = area boundary, λ = constant, R = radius of considered area.

Using the static solution from LEFM, expressions for the energy terms can be derived. (See Appendix). Substitution leads to the result that the balance is a function of load, crack size, crack velocity, known constants and one unknown proportionality constant λ.

Presentation of the mathematical formalism and discussion of the various energy terms exceeds the scope of this paper. These are given in [19]. To indicate the nature of the final result for the energy balance, it can be written, like the result of Mott and Berry, as a quadratic equation of $\dot{a}$:

$$AA(t)[\dot{a}(t)]^2 + BB(t) + \dot{a}(t) + CC(t) = 0. \tag{5}$$

In this equation the first two terms are mainly determined by the kinetic energy.

To determine the unknown constant λ, the analytical expressions for the work $W(t)$ and the deformation energy under static loading $V(t)$ of Sneddon [20] are used. λ equals 0.56 for a Poisson's ratio of 0.25. Assuming that the size of the fracture zone is not affected by the loading rate, the crack extension can be determined by solving (5).

Some results are presented in Figs. 3 and 4 [19]. Figure 3 shows the crack growth of one single crack, in case the stress fields are adjusted by the function $k(a)$ or not. The crack growth in the fictitious plane for various loading rates is given in Fig. 4.

From these results it emerges that for low loading rates the limiting velocity for a single crack is the Rayleigh wave, as it should be, but that the terminal crack velocity decreases with increasing loading rate. When the finite geometry of the fictitious fracture plane is considered, the same feature is observed for the rate dependency (Fig. 4). Calculations showed that the velocity decreases with decreasing intermediate crack distance. This aspect emerges also from a comparison of Figs. 3a and 4a.

3.3. Discussion of results

From the results presented in the former section, it is concluded that at least for low loading rates the crack extension model gives reliable results as the terminal crack tip velocity equals C_r. For higher loading rates the result is not directly obvious. An analysis of the effect of the loading

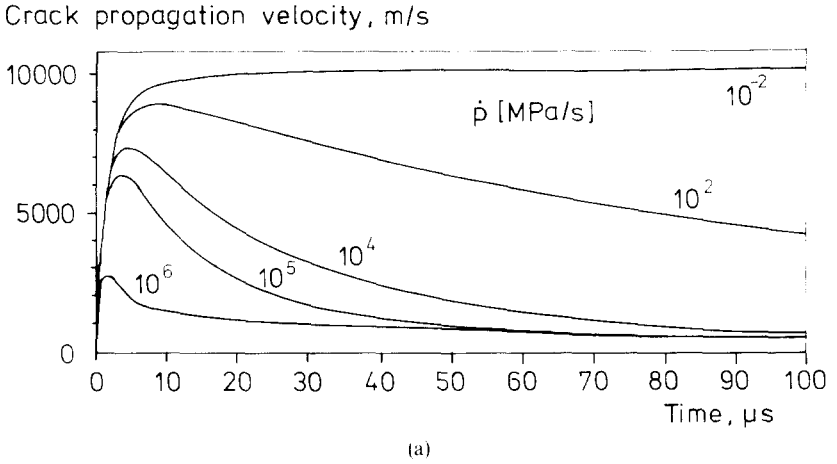

(a)

Fig. 3. Velocity of crack extension for various loading rates $\dot{p}$ for one crack. $\dot{p} = 10^{-2}, 10^2, 10^4, 10^5, 5 \cdot 10^5, 10^6$ MPa/s. (a) No adjustments for inertia effects. (b) Adjustments for inertia effects.

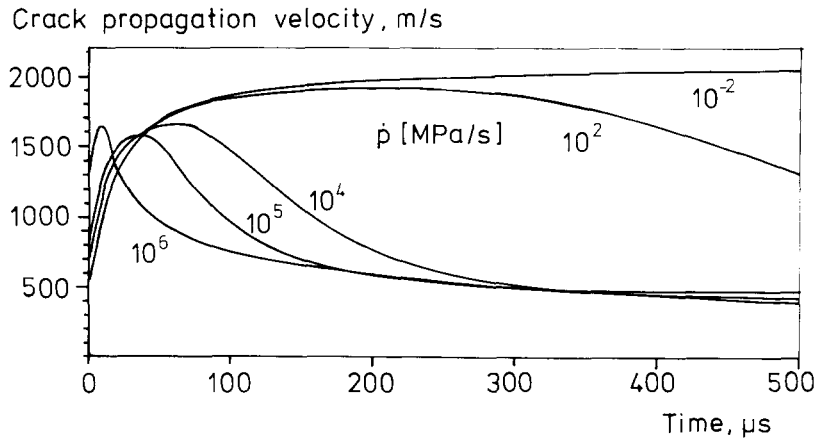

(b)

Fig. 3.—contd.

rate on the various energy components showed that the kinetic and deformation energy, normalized by the work, increased significantly with increasing loading rate. It seems that the rate of energy supply can become too high to be absorbed in the fracture process, resulting in an equilibrium in which a major part of the energy supplied is stored around the crack tip as kinetic and deformation energy. This should mean that the stress distribution around the crack tip changes and the stress intensity factor decreases with increasing loading rate due to the contribution of the inertia to the force equilibrium. This is the same result as Curbach [10] obtains from his finite element calculation on a notched specimen. It may be noted also that there is support for the foregoing results from the damage model of Chen [21].

Finite geometry affects the kinetic energy terms through the velocity field during crack extension (see Appendix.) In (5) the functions $AA(t)$ and $BB(t)$ increase with decreasing intermediate distance resulting in an equilibrium at a lower crack velocity.

It should be noted that the results of Fig. 4b show that the mean crack tip velocity increases in the fictitious fracture plane with increasing loading rates. This feature is consistent with experimental observations for macro cracking in [22] and [10].

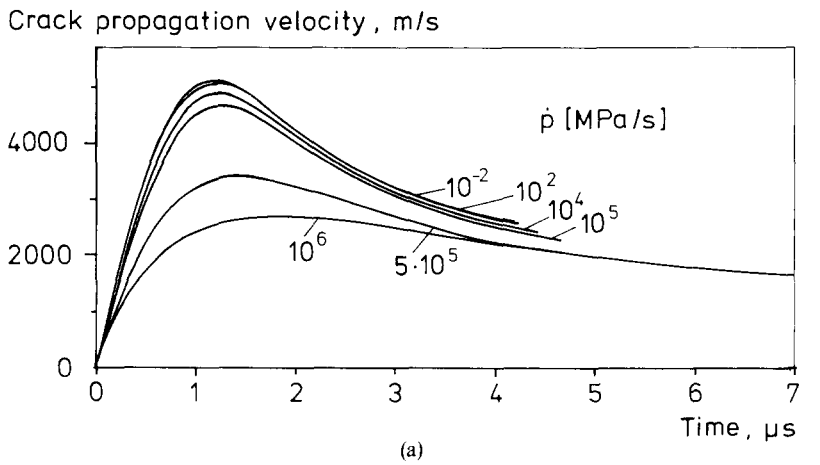

(a)

Fig. 4. The velocity of crack extension for various loading rates $\dot{p}$, and finite geometry ($a_0/b = 0.4$, see Fig. 1). $\dot{p} = 10^{-2}$, 10^2, 10^4, 10^5, $5 \cdot 10^5$, 10^6 MPa/s. (a) No adjustments for inertia effects. (b) Adjustments for inertia effects.

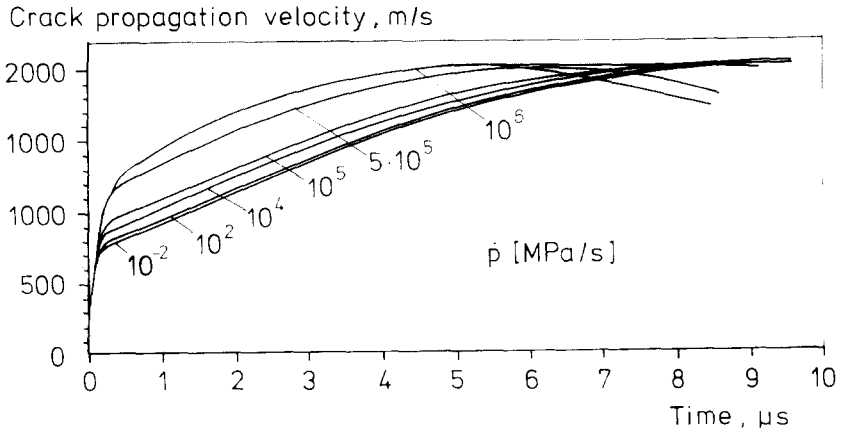

(b)

Fig. 4. —contd.

In the following section the crack extension model will be applied to the schematic failure plane for concrete.

4. Comparison of model prediction with test results

To determine the effect of the loading rate on the failure process and the tensile strength, crack propagation for various loading rates is compared with the process under static loading. Because no micro cracking, crack arrest or branching are modelled, no absolute values for the crack velocity or strength can be obtained without reference to the values under static loading. The rate effect on the strength follows from relating the processes modelled under dynamic and static loading [19].

To show how the effect of the model and loading rate on the crack extension is reflected in the dynamic tensile strength, first the fracture energy will be kept constant. Figure 5 shows the results for a high (A) and a low (B) quality concrete together with some experimental data. The difference in quality is characterized by a factor two in compressive strength. The lines A and B in Fig. 5 show that the model predicts the strength increase for high loading rates very well and also the more sensitive response for lower concrete quality.

From this result it must be concluded that the steep strength increase for high loading rates is not caused by an increase in fracture energy due to a different fracture path or multiple cracking, but is caused by a changing stress and energy distribution in the regions around the crack tip. From this result it emerges also that the increase at lower loading rates is caused by increasing energy demand, which has to be included in the model. Zielinski [23] studied the different fracture planes and multiple cracking under dynamic loading. His work has been used to incorporate these effects on the geometry of the fictitious fracture plane and the stress field. The results are given in the lines A' and B' of Fig. 5.

With this approach the predicted dynamic strength corresponds well with the experimental data for rates from 10^{-2} to 10^{6} MPa/s. The effect of concrete quality is also represented well for the lower rates.

The phenomena described by the model are well known. For instance, the crack and damage extension at high strain rates led to the cube root relation of Kipp (3); recently Curbach applied

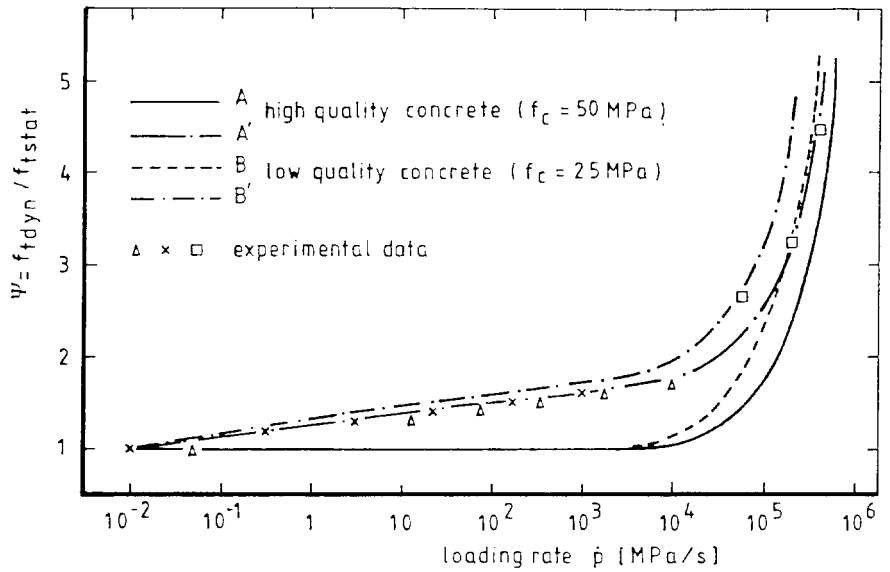

Fig. 5. Relative tensile strength $\Psi(=f_{td}/f_{ts})$ as a function of the loading rate $\dot{p}$. Experimental results from Zielinski [23], Takeda [24], and Birkimer on medium and low strength concrete.
Line *A*: high quality concrete; constant fracture energy.
Line *A'*: high quality concrete; fracture energy depends on p.
Line *B*: low quality concrete; constant fracture energy.
Line *B'*: low quality concrete; fracture energy depends on p.

the experimentally determined maximum velocity for macro cracks to explain the steep strength increase in the high rate region. The main inertia effect on material response, i.e. the limiting damage extension rate was also applied in the first version of the current model [25]. The newer work however reflects a more basic approach, using the conservation of energy; it led to an expression for damage extension process for all loading rates. Thus, the model offers the opportunity to examine the influence of concrete composition and material properties on the fracture process and, in particular, impact on dynamic strength.

5. Concluding remarks

It can be concluded that the moderate and steep increase of the tensile strength between low and high loading rates are caused by two different phenomena. For loading rates up to about 10 GPa/s the strength increase is caused by an increasing energy demand to form the final fracture plane. Aggregate fracture and multiple fracture occurs. The mechanism of the extension of the existing damage does not change for these loading rates and the dependency can be expressed as a power function with one constant coefficient (see Eqn. (2) of [6]). The steep increase beyond 10 GPa/s is caused by a mechanical response of the materials around the crack tip in which the inertia effects become dominant. The distribution of the energy supplied changes and K_{ID} decreases, thus causing a decreasing crack propagation velocity and a corresponding increase in strength.

The crack extension in the fictitious fracture plane showed that the crack velocity in linear elastic material is limited to the Rayleigh wave velocity but also that the terminal crack velocity

decreases at higher loading rates to about $0.25\,C_r$. Comparison of this result with the observed crack velocities in real concrete is not justified because these are related to macro cracking in the post-peak fracture process in the non-linear and non-elastic material. However, the feature of decreasing terminal velocities at higher loading rates, and so increasing strength, remains valid.

In (1) the fracture energy G_F is coupled to the tensile strength under the condition that no multiple cracking occurs in the measured length of the fracture zone. The aspect of multiple cracking and the determination of G_F from dynamic tests is also discussed in [26]. From the different mechanisms indicated by the model, it emerges that (1) can only be valid for moderate loading rates, because for higher loading rates the rate dependency of the strength is not coupled to the dissipated fracture energy.

Finally, in spite of the assumptions and simplifications, the model describes well the rate dependency of the uniaxial tensile strength for all loading rates and reflects also the rate sensitivity for different concrete qualities. Apparently the most important aspects of the material response of concrete under dynamic loading, but before ultimate load, can be characterized by the extension of the existing damage in the fictitious fracture plane.

Appendix: The energy terms

The terms are given by:

- The work $W(t)$ is determined by the stress component, normal to the surface A and the displacement of the material at the envelope.

$$W(t) = \iint_A (\sigma_n,\, \mathrm{d}u)\,\mathrm{d}A,$$

where σ_n is the component of the stress vector normal to the surface A and $\mathrm{d}u$ is a component of the differential of the displacement vector.

$$W(t) = 2\frac{(1+\nu)}{E}\cdot CV_t \int_t [p\dot{p}af^2 + \frac{p^2a}{2}(f^2 + fg)]\,\mathrm{d}\tau,$$

with ν = Poisson's ratio, p = loading, f = geometry function, E = Young's modulus, $\dot{p}$ = loading rate, g = geometry function.

The deformation energy $V(t)$ in A is determined by the stress and deformation fields, and follows from volume integration of the vector product of both components.

$$V(t) = 0.5 \int_V \sigma\cdot\varepsilon\,\mathrm{d}V,$$

where ε is the strain vector and V the volume inside A.

$$V(t) = \frac{(1+\nu)}{E}\cdot CV_t\cdot p^2af^2.$$

Also the kinetic energy is stored inside A and can be determined when the velocity field is known.

$$T(t) = 0.5\rho \int_V (\dot{u})^2 \, dV,$$

with ρ the density of the material and u the velocity.

$$T(t) = \frac{(1+\nu)^2}{E^2} \cdot \rho \cdot CT_t \left[a\dot{p}^2 f^2 + p\dot{p}\dot{a}(f^2 + fg) + \frac{p^2}{4a}\dot{a}^2(f+g)^2 \right].$$

- The fracture energy $D(t)$ is proportional to the specific surface energy γ and the area of the created fracture planes. For penny-shaped cracks $D(t)$ is given by

$$D(t) = 2 \cdot \gamma \cdot \pi \cdot a^2.$$

In these expressions the coefficients CV_t and CT_t are the result of the surface and volume integrals and given by

$$CV_t = CV(t) = (5aR + 2R^2) - \nu(8aR + 4R^2),$$

$$CT_t = CT(t) = \left(\frac{38}{3} - 32\nu + \frac{64}{3}\nu^2\right) aR^3 - R^4(3 - 4\nu),$$

with $R = \lambda$ times characteristic length.

References

1. R. John and S.P. Shah, Mixed mode fracture of concrete subjected to impact loading, NSF-ACBM Report, Northwestern University, Evanston, January 1989, 1–18.
2. A. Hillerborg, *International Journal of Cement Composites* 2 (1980) 177–184.
3. D.A. Hordijk and H.W. Reinhardt, in *Brittle Matrix Composites* 2, A.M. Brandt and I.H. Marshall (eds.), Elsevier Applied Science Series, London (1988) 486–495.
4. H.A. Kormeling and H.W. Reinhardt, *International Journal of Cement Composites and Lightweight Concrete* 9 (1987) 197–204.
5. A.S. Krausz and K. Krausz, *Fracture Kinetics of Crack Growth*, Kluwer Academic Publishers, Dordrecht (1988).
6. H. Mihashi and F.H. Wittmann, *Heron* 25 (1980) 1–54.
7. M.E. Kipp, D.E. Grady and E.P. Chen, *International Journal of Fracture* 17 (1980) 471–478.
8. S.P. Shah and R. John, in *Fracture Toughness and Fracture Energy of Concrete*, F.H. Wittmann (ed.), Elsevier, Amsterdam (1986) 453–465.
9. D. Muria Vila and P. Hamelin, in *Proceedings 1st RILEM Congress* 2, Chapman & Hall, London (1987) 725–732.
10. M. Curbach, Festigkeitssteigerung von Beton bei hohen Belastungsgeschwindigkeiten, Dr.-Ing. dissertation, Karlsruhe, Germany, 1987.
11. J. Weerheijm, Schematisation of the fracture process in concrete under compressive and tensile loading, Research report TNO-PML No. 1987-16, Delft (1987) in Dutch.
12. L.B. Freund, *Journal of the Mechanics and Physics of Solids* 21 (1973) 47–61.
13. K.B. Broberg, *Arkiv fur Fysik* 18 (1960) 159–192.
14. C. Atkinson and J.D. Eshelby, *International Journal of Fracture Mechanics* 4 (1968) 3–8.
15. J.D. Achenbach and L.M. Brock, in *Dynamic Crack Propagation*, G.H. Sih (ed.), Noordhoff, Leyden (1972).

16. H. Nozaki et al., *International Journal of Solids and Structures* 22 (1986) 1137–1147.
17. N.F. Mott, *Engineering* 165 (1948) 16–18.
18. J.P. Berry, *Journal of the Mechanics and Physics of Solids* 8 (1960) 194–206.
19. J. Weerheijm, Properties of Concrete Under Dynamic Loading 3. Fracture Model for Brittle Materials, PML 1990–9, Rijswijk (1990).
20. I.N. Sneddon, in *Mechanics of Fracture 1. Methods of Analysis and Solutions of Crack Problems*, G.C. Sih (ed.), Noordhoff, Leyden (1973).
21. E.P. Chen, in *Proceedings Symposium on Cement-Based Composites: Strain Rate Effects on Fracture*, Materials Research Society Symposium Proceedings 64 (1986) 63–77.
22. R. John and S.P. Shah, A fracture mechanics model to predict the rate sensitivity of mode I fracture of concrete, Northwestern University, Evanston, November 1986.
23. A.J. Zielinski, *Fracture of Concrete and Mortar Under Uniaxial Impact Tensile Loading*, Delft University Press, Delft (1982).
24. J. Takeda and H. Tachikawa, in *Proceedings International Conference on Mechanical Behaviour of Materials*, Kyoto IV (1971) 267–277.
25. J. Weerheijm and W. Karthaus, in *Proceedings Symposium on The Interaction of Non-Nuclear Munitions with Structures*, Panama City Beach (1985).
26. J. Weerheijm and H.W. Reinhardt, in *First International Conference on Structures Under Shock and Impact*, Cambridge, Massachusetts (1989).